

# Insight into the Molecular Arrangement of High-Density Polyethylene Polymer Chains in Blends of Polystyrene/High-Density Polyethylene from Differential Scanning Calorimetry and Raman Techniques

JAYANT JOSHI, RICHARD LEHMAN,\* and GENE S. HALL

AMIPP Advanced Polymer Center, Rutgers University, 607 Taylor Road, Piscataway, New Jersey 08854 (J.J., R.L.); and Department of Chemistry and Chemical Biology, Rutgers University, 610 Taylor Road, Piscataway, New Jersey 08854 (G.S.H.)

Polystyrene/high-density polyethylene (PS/HDPE) blends were synthesized by melt blending in a single screw extruder. Co-continuity measurements using solvent extraction and scanning electron (SEM) micrographs showed that co-continuity was obtained around 35% PS. Thermal analyses measurements revealed a reduction in crystallinity of the HDPE phase around the co-continuous composition. Raman analyses across the entire composition range of these blends showed an increase in the normalized integral intensities of the 1128 cm<sup>-1</sup> and 1061 cm<sup>-1</sup> stretching vibrations of the HDPE molecules. The presence of all-trans HDPE chains that are not packed into an orthorhombic structure is used to explain the simultaneous occurrence of reduced crystallinity and increased intensity of all-trans HDPE stretch vibrations.

Index Headings: Blends; Raman; Polyethylene; Polystyrene.

## INTRODUCTION

The process of solidification from the melt state in polymers involves numerous transformations at the molecular level. Crystallization in semi-crystalline polymers is one of the most important of these transformations, which proceeds via the rearrangement of chains into regular three-dimensional structures called lamellae.<sup>1</sup> In polyethylene, these lamellae can form polymorphic crystals with an orthorhombic or monoclinic structure depending on the thermal and mechanical history of the polymer. At room temperature and atmospheric pressure, the orthorhombic structure is the most stable form of packing. The characteristics of the polymer crystallizing into this lamellar structure can be analyzed using various analytical techniques such as Raman,<sup>2</sup> differential scanning calorimetry (DSC),<sup>3</sup> tunneling electron microscopy (TEM),<sup>4</sup> small-angle X-ray scattering (SAXS),<sup>4</sup> atomic force microscopy (AFM),<sup>4</sup> nuclear magnetic resonance (NMR),<sup>5</sup> and Fourier transform infrared (FT-IR) spectroscopy.<sup>6</sup> The use of Raman spectroscopy to quantify the crystalline phase of polyethylene was first developed by Strobl and Hagedorn.<sup>2</sup> The relative intensity of the 1415 cm<sup>-1</sup> polyethylene phase was used by them and others<sup>7-9</sup> to quantify the degree of crystallinity and crystalline structure packing of the polyethylene phase. This Raman band results from crystal field splitting of the two components of the methylene bending vibration, which occurs only when the unit cell is occupied by two structural units, as in an orthorhombic lattice. In two-phase polymer blends, such as those generated by immiscible polymer composites, the process of crystallization is substantially altered by the spatial and mechanical interaction between the two phases, as has been demonstrated

by DSC crystallinity measurements. Such investigations have shown wide variations in specific composition regions of immiscible polymer blends,<sup>10-12</sup> and studies in our laboratories have shown that immiscible blends of polystyrene/high-density polyethylene (PS/HDPE) and polystyrene/polypropylene (PS/PP) show a characteristic reduction in the crystallinity of the semi-crystalline component in their co-continuous region.<sup>13</sup> These variations have been explained only qualitatively from the perspective of inter-domain mechanics and a fundamental understanding of this process with regard to polymer molecular mechanisms is lacking.

In this paper, we have studied changes in the Raman spectra of PS/HDPE blends to assist in defining the molecular rearrangement of the HDPE phase in the enigmatic co-continuous region. Results from these studies have been combined with DSC data to promote the understanding of the molecular rearrangement of polymer chains in this particular area of the PS/HDPE composition range.

## EXPERIMENTAL

**Materials.** A general purpose polystyrene (GPPS7 GE Polymerland) and an extrusion-grade high-density polyethylene (HHM 5202 BN Chevron Phillips Chemical Co., LP, Houston, TX) were selected for preparation of the blends by melt extrusion. Properties of the virgin polymers, as provided by the supplier, are shown in Table I.

**Rheology and Blend Formulation.** Both polymers were rheologically characterized over a range of shear rates at 200 °C, the relevant processing temperature, to define their viscosity behavior during subsequent extrusion. All measurements were performed using a TA AR 2000 rheometer (TA Instruments, New Castle, DE). Viscosity data are necessary to determine the composition range at which co-continuous blends occur. The composition range for such blends, which typically have the best properties due to their intertwining networks, can be approximated by various methods. One such method given by Jordhamo<sup>14</sup> identifies the region according to the following relationship between the volume fraction ( $\Phi$ ) ratio and the viscosity ( $\eta$ ) ratio of the components at the processing temperature:

$$\frac{\eta_A}{\eta_B} \cong \frac{\Phi_A}{\Phi_B} \quad (1)$$

Although such relationships are useful, the entire range of compositions was of interest in this study, and estimates of co-continuous compositions were only made in order to cluster compositions in the expected ranges.

Received 20 January 2006; accepted 21 February 2006.

\* Author to whom correspondence should be sent. E-mail: rllehman@rutgers.edu.

**TABLE I. Properties of the virgin polymers.**

Polymer	Melt flow data					
	Index (g/10 min)	Load (kg)	Temperature (°C)	Density (g/cc)	Tensile yield (MPa)	Flexural modulus (MPa)
Extrusion-grade high-density polyethylene	0.35	2.16	190	0.952	27	1309
Virgin-grade polystyrene	7.0	5.0	200	1.04	53.78	3317.00

**Blend Synthesis and Thermal Analyses.** The test materials were extruded in a 17 mm single screw extruder (C. W. Brabender Instrument Corporation, Hackensack, NJ) at 200 °C and at 100 rpm. DSC tests were performed on all compositions using a standard heat ramp procedure between 40 and 240 °C at a ramp rate of 10 °C/min. The DSC tests were performed on a TA Q-1000 calorimeter (TA Instruments, New Castle, DE).

**Electron Microscopy.** Small rectangular sections from the test specimens were cryo-fractured in liquid nitrogen to obtain a surface with preserved morphology. Most samples were etched with toluene for 15 minutes to extract polystyrene to improve imaging. After drying overnight, the samples were sputter-coated with gold and analyzed in a Leo-Zeiss Gemini 982 field emission scanning electron microscope at a voltage of 5 keV.

**Raman Spectroscopy.** Room temperature (21 ± 1 °C) Raman spectra were obtained from a Renishaw (Renishaw Inc., Hoffman Estates, IL) System 1000 dispersive micro-Raman spectrometer. The system has a 785 nm diode laser for illuminating the sample and a holographic notch filter to minimize the Raleigh scattered line. The Raman photons were focused onto a 1200 lines/mm holographic grating and sent to a Peltier charge-coupled device (CCD) detector for analysis. The laser intensity at the sample was 25 mW and we used a line focus lens to project the laser onto the sample via a 50× objective lens from the Leica microscope. This line focus lens produced a 2 × 40 μm homogeneous laser beam profile on the sample so that a representative sample area was illuminated. We used 4-acetamidophenol (ASTM Designation: E 1840-96) to calibrate the Raman spectrometer over the data collection range of 1600 to 900 cm<sup>-1</sup> at 2 cm<sup>-1</sup> resolution.

The micro-Raman spectrometer is equipped with a computer controlled x, y, z stage. Under the control of Renishaw Wire 2.0 data acquisition software, we used this instrumental configuration to map a 100 μm long line-scan region across the sample and analyzed ten step scans at 5 μm increments in the sample. Data acquisition consisted of three 20 s accumulations per step scan that were coadded to form an averaged data point per sample. The ten averaged Raman spectra per sample were averaged to form a single composite spectrum that was used in plotting the graphs and in interpreting the data.

## RESULTS AND DISCUSSION

**Viscosity and Blend Composition.** The predicted co-continuity composition region for different shear rates is shown in Fig. 1 along with the viscosity values for both PS and HDPE as a function of shear rate. The shear rate in the Brabender extruder is nominally ~80 s<sup>-1</sup> at 100 rpm, although various mixing elements on the screw and other sources of variability can provide shear rate values within an estimated band of this nominal value ±50%. The highlighted region in the curve represents the nominal shear rate in this range. Also highlighted is the range of composition at which co-continuous

blends are anticipated based on the viscosities and the Jordhamo relationship. Hence, the expected co-continuity region is near 34% PS by volume (36% by weight). However, since the viscosity curves for both polymers are nearly parallel over a wide range of shear rates, we expect co-continuous morphologies to be observed near 34% PS almost independent of the actual shear rate.

**Scanning Electron Microscopy Observations on Morphology.** Scanning electron microscopy (SEM) photomicrographs of blend sections cut perpendicular to the extrusion axis for all compositions in the experimental range are shown in Fig. 2. At 30% PS the blends show a dispersed PS phase morphology with a nearly circular cross-section. By 35% PS, these features become slightly elongated and at 40% PS composition, the blend is seen to achieve a co-continuous structure, which persists at the 45% composition. At 50% PS composition, the structure appears collapsed with respect to the HDPE matrix, which suggests that HDPE is no longer a continuous structure at this composition. The unetched 60% PS composition shows dispersed HDPE domains in a matrix of PS.

The elongation of PS domains observed at 35% PS composition is of importance as it points to an induced orientation in the domains of the blend. This effect will be shown in later sections to have important effects on the molecular orientation of the polymer chains. To substantiate our observations of co-continuity around the 40% PS composition, we used solvent extraction to selectively etch out the PS phase and measure the weight loss in the extraction process. The degree of continuity was measured using the following formula:

$$\text{Degree of continuity} = \left[ \frac{(\text{initial mass of PS} - \text{remaining mass of PS}) \times 100}{\text{initial mass of PS}} \right] \quad (2)$$

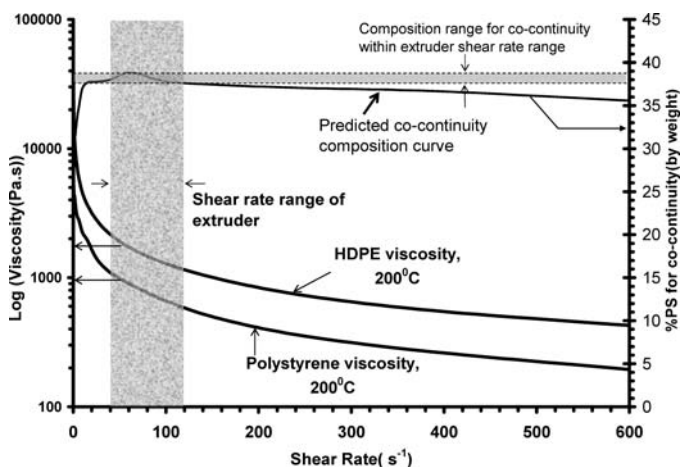


Fig. 1. Viscosity dependence of shear rate of polystyrene and HDPE resins and range of co-continuous compositions predicted by Jordhamo's relationship.

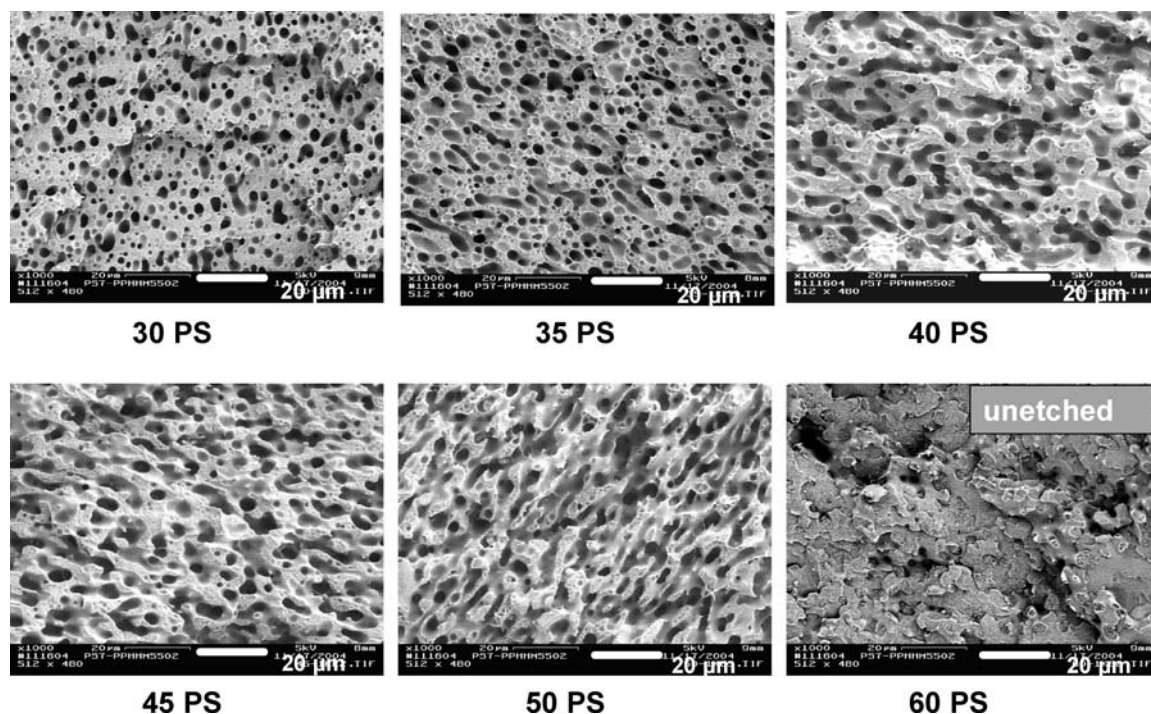


FIG. 2. SEM micrographs of PS/HDPE blends as a function of composition.

The measured degree of continuity (DOC) of the PS phase in Fig. 3 indicates very little solvent access to the PS phase at compositions below 20% PS, at which composition less than a tenth of the polystyrene in the blend is removed by solvent. In the 20–30% PS region, a sharp increase in DOC is observed and by 35% PS a fully co-continuous structure is observed by virtue of the fact that virtually all (~98%) PS in the blend is accessible to the solvent and is removed.

The SEM observations, however, do not reveal complete continuity until the 40–45% PS composition is reached. The difference between the SEM image analysis and the DOC solvent extraction measurements seems certainly due to the accessibility of the PS phase as the composite progresses from a completely discrete composite at very low levels of PS to the three stages of co-continuity: uniaxial (one dimensional), biaxial (two dimensional), and network co-continuity, i.e., full

three-dimensional co-continuity. Traditionally, the three-dimensional network co-continuity has been the structure characterized as co-continuous and it is this structure that the SEM photomicrographs illustrate at 40–45% PS. However, at much lower PS volume fractions the PS become co-continuous in one dimension, thus permitting some degree of solvent access to the polystyrene, assuming transport and saturation effects can be overcome. Only when the polystyrene is at very low volume percentage, e.g., <15%, is the PS a fully discrete phase and accessible to solvent extraction only at very low levels via surface dissolution. Thus, the DOC measurements are expected to over-estimate the degree of network co-continuity at compositions of PS/HDPE below that corresponding to true network co-continuity. Curiously, the Jordhamo relationship predicts network co-continuity for this system in the range of 37–39% PS, precisely where the DOC curve intersects 100% continuity, suggesting that the development of co-continuity is indeed a process that occurs over a composition range and which yields slightly different results depending on the method of characterization. In this work, the confluence of the Jordhamo prediction with SEM and DOC measurements has provided us with confidence that network co-continuity begins to develop near 25% PS and is fully developed by 40–45% PS.

**Differential Scanning Calorimetry Observations.** Differential scanning calorimetry measurements were done on all the blends in a heat ramp cycle and the crystallinity was measured using the area under the melting peaks. Figure 4 shows a drop in crystallinity at 35% PS composition and remains roughly constant between the 35% and 45% PS composition, followed by an increase beyond the 50% PS composition range. The reduction in the crystallinity around the 35% PS composition is indicative of an inhibited crystallization process in the corresponding blends and is a subject of the present research. This reduction has been observed in the past, especially for co-continuous immiscible blend structures,<sup>13</sup> and has been

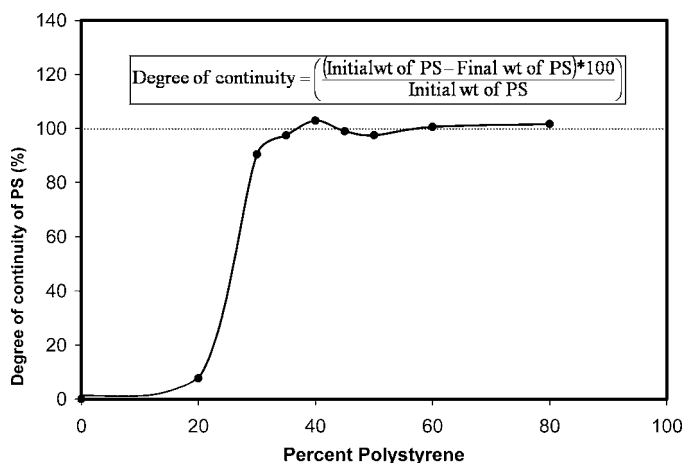


FIG. 3. Solvent extraction results on PS/HDPE blends for measurement of co-continuity of the PS phase.

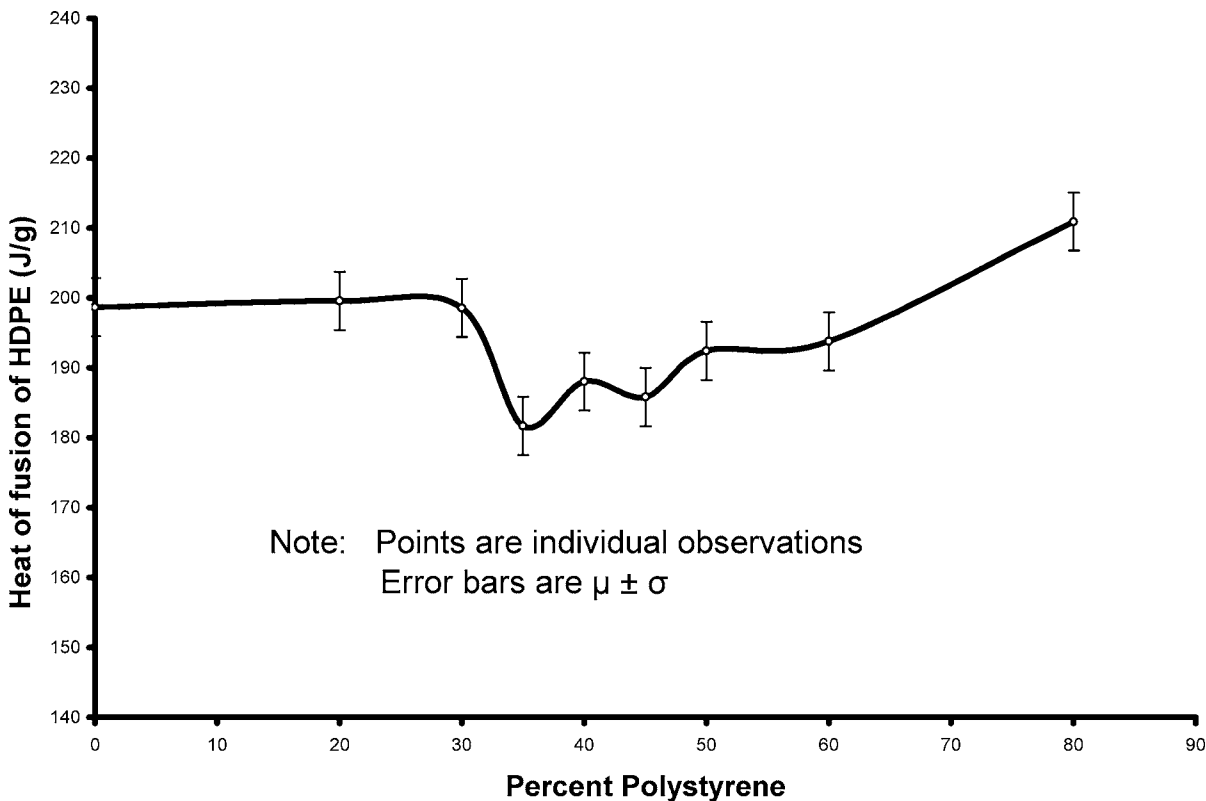


FIG. 4. Crystallinity variation of the HDPE phase measured using DSC in PS/HDPE blends.

explained by observing the fact that the fineness of the HDPE domains at these compositions influences the crystallization behavior of the polymer when solidifying from the melt state.

This anomalous reduction in crystallinity is related to Raman spectroscopic observations, as shown in the sections that follow, and gives a possible mechanism of the inhibited crystallization process that occurs at these compositions.

**Raman Spectroscopic Observations.** The Raman spectra

of PS, HDPE, and their blends are shown in Fig. 5. For each composition, ten sampling points were taken and the integral intensities of peaks were measured using analytical software. The peaks of interest in HDPE and PS are tabulated in Table II with the respective band assignments.

The Raman spectrum of HDPE can be roughly divided into three regions as shown in Fig. 6. The C–C stretching vibration belongs to the first region ( $1040\text{--}1160\text{ cm}^{-1}$ ), the  $\text{CH}_2$  twisting

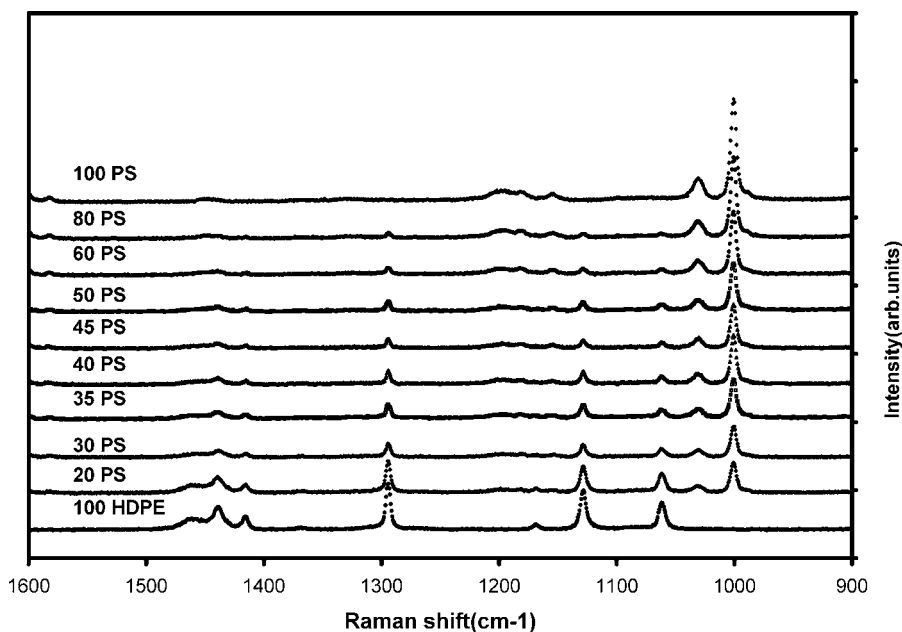


FIG. 5. Raman spectra of PS/HDPE blends as a function of composition.

**TABLE II. Band assignments to characteristic Raman frequencies of polystyrene and HDPE polymers.**

Raman shift wavenumber (cm <sup>-1</sup> )	Vibrational mode (HDPE)	Vibrational mode (PS)
1001 (PS)		In-plane ring def. + out-of-plane CH deformation
1030 (PS)		In-plane CH deformation
1061 (HDPE)	Out-of-phase C–C stretching vibration of all-trans alkyl chains of HDPE	
1128 (HDPE)		
1154 (PS)		In-plane CH deformation
1181 (PS)		In-plane CH deformation
1198 (PS)		In-plane CH deformation
1294 (HDPE)	In-phase CH <sub>2</sub> twist	
1415 (HDPE)	Methylene bending vibration	
1439 (HDPE)	Methylene bending vibration	

vibrations to the second region (1250–1340 cm<sup>-1</sup>), and the CH<sub>2</sub> bending vibrations belong to the third region (1390–1510 cm<sup>-1</sup>) of the spectrum.<sup>2</sup> The C–C stretching vibrations at 1128 and 1061 cm<sup>-1</sup> are known to arise from all-trans conformations of HDPE chains. Crystalline PE is known to be formed by all-trans chains of polyethylene, and hence the bands at 1128 and 1061 cm<sup>-1</sup> could as well be used for quantification for the level of crystallinity. However, these bands arise from the all-trans alkyl chains, some of which may not necessarily belong to crystalline HDPE. Previous studies have shown that all-trans sequences that contribute to the two intensities may also be present in an oriented amorphous state.<sup>15</sup> Strobl and Hagedorn<sup>2</sup> also discuss the existence of these all-trans chains of HDPE, which show no packing in the lateral direction, and the presence of such chains has also been confirmed in subsequent studies.<sup>7</sup> Thus, we expect contributions to these stretching intensities from all those portions of HDPE chains that are in trans conformation, i.e., not present at fold junctions, and from trans chains in oriented HDPE.

To map out the intensity variations in the stretching vibration region of the spectrum across the entire composition range of

our blends, an internal standard for normalizing the peaks was required. Such an internal standard is provided by the integral intensity of the 1294 cm<sup>-1</sup> peak, as suggested by Strobl and Hagedorn, who demonstrated that the scattering power of this twisting vibration is independent of chain conformation and hence can serve as an internal standard for all other intensities. To investigate the feasibility of using the 1294 cm<sup>-1</sup> peak as an internal standard, its integral intensity was plotted as a function of composition for all the blends (Fig. 7). The intensity is seen to decrease over the entire composition region except for a slight increase at 50% PS composition. This increase is also observed in all the other vibrational peaks mapped and is attributed to surface area effects resulting in increased scattering cross-sections at this composition. Such effects are canceled out in the ratios of the relevant peaks with the 1294 cm<sup>-1</sup> peak, and hence this peak serves as a good standard for all other peaks.

The normalized intensities of the 1128 and 1061 cm<sup>-1</sup> peaks with respect to the 1294 cm<sup>-1</sup> peak are shown in Figs. 8 and 9. An interesting observation arises here, namely that both the in-phase and out-of-phase C–C stretch vibrations are enhanced at

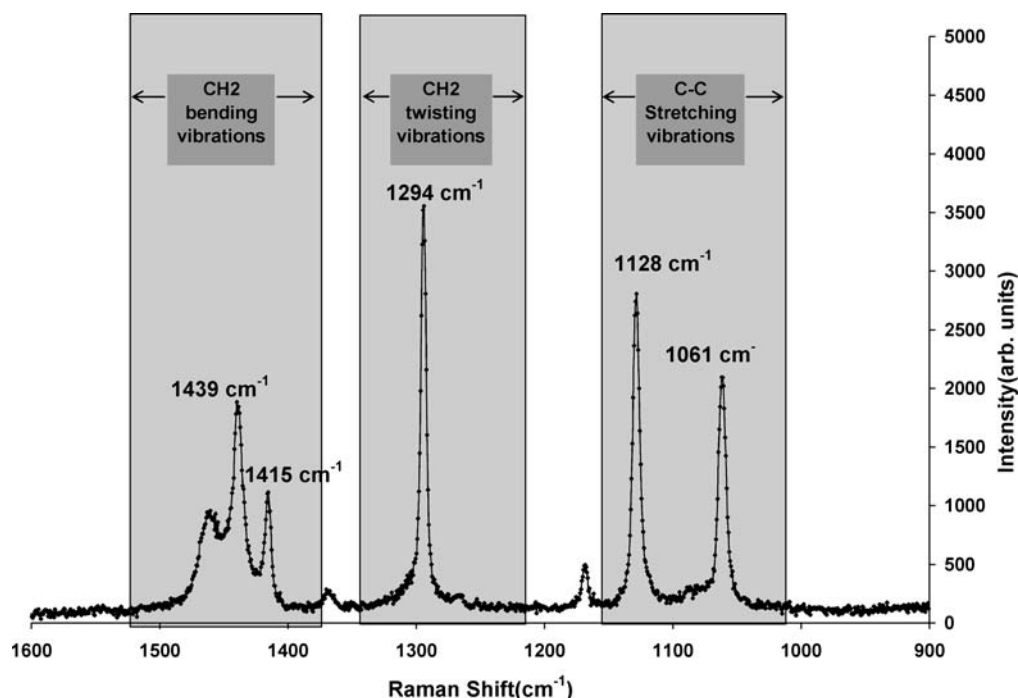


Fig. 6. Raman vibrational spectrum of HDPE with some band assignments.

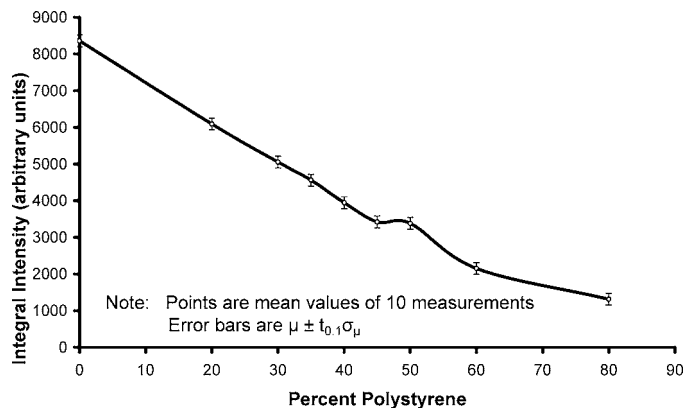


FIG. 7. Integral intensity variation of the  $1294\text{ cm}^{-1}$  vibrational frequency as a function of composition.

the 35–45% PS/HDPE composition, while at the same composition the crystallinity of HDPE appears to be reduced. The  $1128$  and  $1061\text{ cm}^{-1}$  bands are very often referred to as crystalline bands, and our observations present a contradiction to this view. The reason for this discrepancy is the presence of all-trans chains without lateral packing, as explained above.

Previous studies have shown that crystalline HDPE is composed of ethylene chains in an all-trans conformation. These chains form an orthorhombic crystalline structure during the process of crystallization. The microstructure plays an important role during the solidification stages of the blend, when the HDPE chains re-orient to pack into their orthorhombic crystalline structure. This spatial arrangement into an orthorhombic lattice involves a lot of chain folding, and the all-trans conformation cannot be retained for bonds at the fold junctions.<sup>15</sup> The observed crystallinity reduction via DSC can be explained by the fact that the domains of the phases near the 35–45% PS/HDPE composition are small in diameter and

significantly elongated because of the specific shear-viscosity relationships between the two polymers. This induces spatial constraints on the HDPE chains and hinders achievement of the folded chain structure of crystals. Such spatial constraints combined with other micro mechanics are the likely cause of the reduction in crystallinity of polyethylene at 35–65% composition. This reduction in crystallinity for compositions approaching co-continuity is not unique to PS/PE, but has been observed in PS/PP blends<sup>16</sup> as well as in recycled PS/HDPE blends.<sup>17</sup>

The structure of crystallized HDPE is well known and is composed of numerous and repeated folding of the polyethylene chains into lamellae. Conversely, when the crystallinity is reduced, the degree to which such chains are folded is reduced. Thus, the average number of HDPE chain folds is reduced in such structures and a greater proportion of the chains are now available to contribute to the C–C stretch vibrations due to the increased fraction of chains retaining their all-trans conformation. This shows up as an increase in the  $1128$  and the  $1061\text{ cm}^{-1}$  peak intensity, as seen in Figs. 8 and 9. The existence of these all-trans chain structures that do not show a packing order in the lateral direction has been shown by Strobl et al.<sup>2</sup> and was later confirmed by others. Strobl et al. used the ratio of the  $1415$  and  $1440\text{ cm}^{-1}$  peaks to prove the existence of these molecular arrangements. These authors showed that the observed enhancement of the  $1415\text{ cm}^{-1}$  intensity relative to the  $1440\text{ cm}^{-1}$  intensity was because of the absence of a lateral packing in some of the polyethylene molecules with all-trans conformation. Our observations show that intensities from these all-trans molecules can be mapped across the entire composition region of the PS/HDPE blends using the  $1294\text{ cm}^{-1}$  integral intensity as a reference. These variations in conjunction with DSC observations reveal an important orientation effect of co-continuous microstructures in the form of an increase in the number of all-trans chains with no lateral packing.

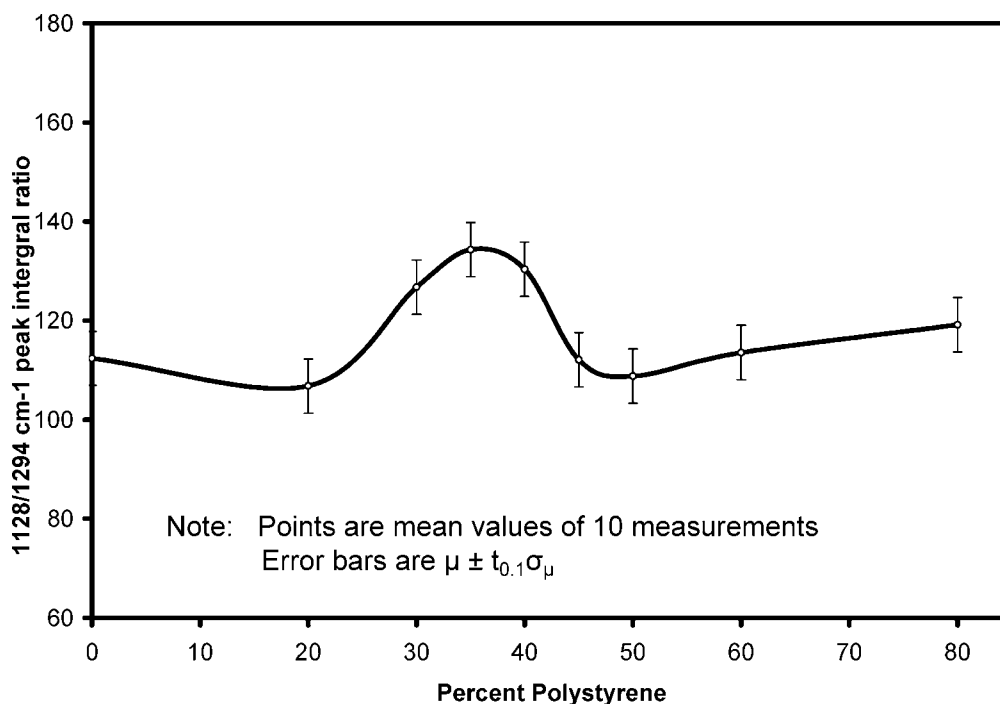


FIG. 8. Integral intensity ratio  $1128\text{ cm}^{-1}/1294\text{ cm}^{-1}$  variation as a function of composition.

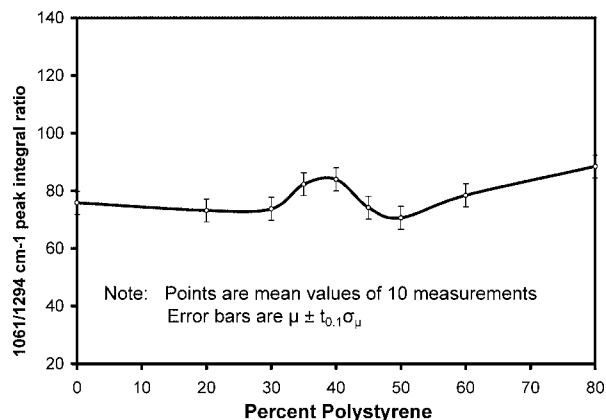


FIG. 9. Integral intensity ratio  $1061\text{ cm}^{-1}/1294\text{ cm}^{-1}$  variation as a function of composition.

## CONCLUSION

Polystyrene/high-density polyethylene blends were synthesized by melt extrusion under modest shear. The blends show network co-continuity near 40% polystyrene composition and a simultaneous reduction of crystallinity of the HD polyethylene phase at the same compositions. Raman observations were obtained over the entire composition region. The integral intensities of the C–C stretching vibrations were plotted after normalizing them to the integral intensity of the  $1294\text{ cm}^{-1}$  phase, which was shown to have a linear reduction with composition. The variations reveal an increase in the intensities around the co-continuous compositions. These intensities are generated by the all-trans portions of the HDPE chains, and normally such chains would be expected to form an orthorhombic crystalline structure. However, the simultaneous reduction of crystallinity and the increase of the all-trans

contributions to the vibrational spectrum show that these chains have not folded into a crystalline structure, and these effects also reveal the strong orientation effects of the co-continuous compositions. The HDPE stretching vibrations are contributions from the straight chains of ethylene, and a reduction of the number of folds in these molecules is shown by the increased normalized integral intensities of these vibrations. These observations reveal a fundamental oriented nature of the molecular arrangements in polymer blends that form co-continuous microstructures.

1. R. Qian, *J. Macromol. Sci., Phys.* **B40**, 1131 (2001).
2. G. R. Strobl and W. Hagedorn, *J. Polym. Sci., Polym. Phys. Ed.* **16**, 1181 (1978).
3. F. M. Mirabella and A. Bafna, *J. Polym. Sci., Part B: Polym. Phys.* **40**, 1637 (2002).
4. H. Zhou and G. L. Wilkes, *Polymer* **38**, 5735 (1997).
5. L. Hillebrand, A. Schmidt, A. Bolz, M. Hess, W. Veeman, and R. J. Meier, G. v. d. Velden, *Macromolecules* **31**, 5010 (1998).
6. G. Akovali and A. Atalay, *Polym. Testing* **16**, 165 (1997).
7. J. M. Lagaron, *J. Mater. Sci.* **37**, 4101 (2002).
8. J. M. Lagaron, *Macromol. Symp.* **184**, 19 (2002).
9. R. P. Paradkar, S. S. Sakhalkar, X. He, and M. S. Ellison, *J. Appl. Polym. Sci.* **88**, 545 (2003).
10. L. R. Veronika and E. Reinsch, *J. Appl. Polym. Sci.* **59**, 1913 (1996).
11. V. M. Nadkarni, V. L. Shingankuli, and J. P. Jog, *J. Appl. Polym. Sci.* **46**, 339 (1992).
12. S. Jose, A. S. Aprem, B. Francis, M. C. Chandy, P. Werner, V. Alstaedt, and S. Thomas, *Eur. Polym. J.* **40**, 2105 (2004).
13. J. Joshi, R. L. Lehman, and T. J. Nosker, *J. Appl. Polym. Sci.* **99**, 2044 (2006).
14. G. M. Jordhamo, J. A. Manson, and L. H. Sperling, *Polym. Eng. Sci.* **26**, 517 (1986).
15. R. J. Meier, *Polymer* **43**, 517 (2002).
16. J. Joshi, R. L. Lehman, and T. J. Nosker, "Mechanical grafting and morphology characterization in immiscible polymer blends", in MRS, Fall (2005).
17. R. W. Renfree, Ph.D. Thesis, Rutgers, The State University of New Jersey, Piscataway, New Jersey (1991).